

Reconstructing Geographical-Spectral Pattern in Cognitive Radio Networks

Husheng Li

Abstract—The geographical-spectral pattern of interruptions from primary users within an area is important for upper layer issues like routing and congestion control in cognitive radio networks. The pattern can be considered as an image and can be recovered from reports of secondary users, like random samples for reconstructing an image. Gibbs random fields are used to model the image by employing an energy function to incorporate correlations between neighboring pixels and *a priori* hyperparameters. Bayesian compressed sensing is then used to reconstruct the image based on the assumption that the image is sparse in a certain transform domain. The performance of the image reconstruction is demonstrated by numerical simulations.

I. INTRODUCTION

Cognitive radio is an emerging technique in the field of wireless communications. In a cognitive radio system, a user without license for a frequency band (called secondary user) is allowed to access the licensed frequency band if users with license (called primary users) are not using this band. Such a cognitive radio system can effectively tackle the problem of underutilization in frequency spectrum. Therefore, it has received intensive study in recent years. When the point-to-point communication techniques become mature, more attention has been paid to networking using cognitive radio links. Due to the significant change in physical layer, many upper layer issues like routing and congestion control should be modified accordingly. Some work has been done for these networking problems. For example, opportunistic routing is introduced into cognitive radio networks [13]. A modified TCP protocol in transport layer is proposed for cognitive radio network in [3].

For networking issues, network-wide information is necessary. For example, in link state routing protocol, the metrics of all links in the network are known to all nodes for optimizing routing paths. In cognitive radio networks, local spectrum sensing is insufficient to provide a network-wide information since only local information is obtained via spectrum sensing.

Motivated by the requirement of network-wide information, we study the reconstruction of geographical-spectral information in cognitive radio networks. If we consider one geographical location as a pixel and represent the intensity of primary users' activity in frequency spectrum using grey levels or colors, then the geographical-spectral information is actually an image (throughout the paper, we equalize the

H. Li is with the Department of Electrical Engineering and Computer Science, the University of Tennessee, Knoxville, TN, 37996 (email: husheng@eecs.utk.edu). This work was supported by the National Science Foundation under grants CCF-0830451 and ECCS-0901425.

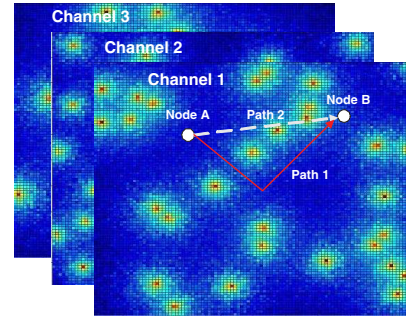


Fig. 1: Illustration of hyperspectral image for cognitive radio.

terms pattern and image. When there are multiple channels or the opportunistic spectrum access is carried out over a wide and heterogeneous frequency band, we can consider the global geographical-spectral pattern as a hyperspectral image¹.

An example of such a hyperspectral image is illustrated in Fig. 1 with three channels. The intensity of the primary users' activity is represented by colors (red means the most intensive while blue means the least intensive). With such a hyperspectral image, the network has full knowledge of the primary users' activity over the whole area.

Although the geographical-spectral information provides little help to physical layer issues like spectrum sensing and data transmission or medium access control (MAC) layer issues like scheduling (both need only local information), it offers a network-wide knowledge about the qualities of different wireless links, thus being significantly helpful for upper layer issues like routing and congestion control. For example, in Fig. 1, when node A sends packets to node B, Path 1, which circumvents the area with intensive activity of primary users, may be better than Path 2 although the Euclidean distance of Path 2 is shorter. In the transport layer, a node can send less packets (e.g. using coarser source coding) to a node located in an area labeled by red color or use a smaller transmission window in TCP.

To reconstruct the network-wide geographical-spectral information, we consider reports from secondary users at different locations (we assume that all secondary users are equipped with GPS and know their location) as random samples in an image and use compressed sensing [2] [4], a novel technique in the field of signal processing, to recover the image. Since it is

¹Hyperspectral image means an image with information from a band of electromagnetic spectrum [5], [10]. It is widely used in mineralogy, military and agriculture.

not necessary to reconstruct all details of the image², it needs only the reports at some locations, based on the assumption that the image is sparse in some linear transform domain and is thus compressible. By reconstructing the image, we can predict the activity of primary users for secondary users not reporting its experience, thus reducing the amount of reports.

To leverage the correlation of adjacent points (in location and spectrum) in the image, we use Gibbs random fields [11] to model this redundancy. Then we apply the technique of Bayesian compressed sensing [8] to convert the problem into a statistical one, with *a priori* information modeled by Gibbs random fields.

The remainder of this paper is organized as follows. Section II will explain the system model. Section III will be devoted to the modeling of the geographical-spectral image using Gibbs random fields. The algorithm to recover the geographical-spectral image, combined with Gibbs random field modeling, will be proposed in Section IV. Numerical results and conclusions will be given in Sections V and VI, respectively.

The following mathematical notation is used throughout the whole paper:

- Kronecker product \otimes : for matrices \mathbf{A} and \mathbf{B} , $\mathbf{A} \otimes \mathbf{B} = (\mathbf{A}_{ij}\mathbf{B})_{ij}$.
- For a matrix \mathbf{X} , $\text{vec}(\mathbf{X})$ means the vector constructed by stacking the columns in \mathbf{X} .

II. SYSTEM MODEL

We consider an $N \times N$ geographical-spectral image³. The observations on the pixels are contaminated with white Gaussian noise having zero mean and variance σ_n^2 . Our purpose is to recover the geographical-spectral image from random samples, i.e. reports from randomly located secondary users, in the image. For simplicity, only one channel is considered.

The following assumptions are used throughout the whole paper.

- Sparsity: we assume that the image is compressible, or equivalently it is sparse under some linear transforms⁴. Otherwise, it is difficult to recover the image.
- Smoothness: we assume that the image is smooth, i.e. neighboring pixels are similar (or equivalently, positively correlated). This is reasonable since typically primary users' activities do not change rapidly in space.
- Processing center: we assume that there is a processing center which collects samples from different locations of the image (equivalently, different secondary users), reconstructs the image and then propagates the image estimation to all secondary users.
- Random deployment: we assume that secondary users are randomly distributed in the image.

III. IMAGE MODELING WITH GIBBS RANDOM FIELD

In this section, we discuss the modeling of the geographical-spectral image using Gibbs random fields. First, we convert

²The purpose of reconstructing the image is to facilitate networking issues, some reconstruction errors do not affect the performance of network.

³It is easy to extend the algorithms, analysis and conclusions to general $N \times M$ images where $N \neq M$.

⁴Sparse means that most elements are zero or close to zero.

the image represented by a matrix into a vector. Then, we propose an energy function to model the correlations. Finally, we incorporate hyperparameters into the energy function.

A. Vectorization

We denote by matrix \mathbf{X} the geographical-spectral image, where each element in the matrix stands for a pixel. Suppose that the image is represented by matrix \mathbf{W} under some two-dimensional transform Φ . Then, we have

$$\mathbf{X} = \Phi \mathbf{W} \Phi^T. \quad (1)$$

By applying Lemma 4.3.1. in [7], which states the equivalence of the following two equations (where \mathbf{A} , \mathbf{X} , \mathbf{B} and \mathbf{C} are all matrices)

$$\mathbf{A} \mathbf{X} \mathbf{B} = \mathbf{C}, \quad (2)$$

and

$$(\mathbf{B}^T \otimes \mathbf{A}) \text{vec}(\mathbf{X}) = \text{vec}(\mathbf{C}), \quad (3)$$

we obtain

$$\mathbf{x} = \Psi \mathbf{w}, \quad (4)$$

where $\mathbf{x} = \text{vec}(\mathbf{X})$, $\mathbf{w} = \text{vec}(\mathbf{W})$ and $\Psi = \Phi \otimes \Phi$.

B. Energy Function for Correlation

Due to the assumption of smoothness, two adjacent pixels in the geographical-spectral image are positively correlated. A powerful tool for modeling the correlation is *Gibbs random fields* [6], [11], [14]. In a Gibbs random field \mathbf{x} , on denoting by x_i the random variable at location i , the joint distribution is given by

$$P(\mathbf{x}) = Z^{-1} \times e^{-\frac{1}{T}U(\mathbf{x})}, \quad (5)$$

where Z is a normalizing factor, T is temperature controlling the level of correlation and $U(\mathbf{x})$ is an energy function. Obviously, when $T \rightarrow \infty$, the energy function does not bring any constraint. We propose to use the following energy function to model the spatial correlation, which is given by

$$U(\mathbf{x}) = \sum_{i \sim j} (x_i - x_j)^2, \quad (6)$$

where $i \sim j$ means that locations i and j are adjacent. It is easy to verify that $i \sim j$ if and only if one of the following conditions holds (suppose that $i < j$):

- Same row, adjacent column:

$$\begin{cases} \mod(i, N) = \mod(j, N) \\ \lceil \frac{i}{N} \rceil + 1 = \lceil \frac{j}{N} \rceil \end{cases}, \quad (7)$$

- Same column, adjacent row:

$$\begin{cases} i + 1 = j \\ \lceil \frac{i}{N} \rceil = \lceil \frac{j}{N} \rceil \end{cases}. \quad (8)$$

Note that, when the pixels are binary, the proposed energy function in (6) is special case of auto-logistic random fields [11], whose energy function is given by

$$U(\mathbf{x}) = \sum_i \alpha_i x_i + \sum_i \beta_{ii} x_i^2 + \sum_{i \sim j} \beta_{ij} x_i x_j. \quad (9)$$

We can rewrite (6) in the vector form, which is given by

$$U(\mathbf{x}) = \mathbf{x}^T \mathbf{J} \mathbf{x}, \quad (10)$$

where

$$(\mathbf{J})_{ij} = \begin{cases} \text{number of neighbors,} & \text{if } i = j \\ -1, & \text{if } i \sim j \\ 0, & \text{otherwise} \end{cases}. \quad (11)$$

C. Energy Function for Geographical-Spectral Image

In the energy function (10), we considered only the correlation between adjacent locations. In order to apply Bayesian compressed sensing, we introduce hyperparameters $\{\alpha_n\}_{n=1,\dots,N^2}$ and consider the energy function (since \mathbf{w} is simply an invertible linear transform of \mathbf{x} , therefore we can also use \mathbf{w} as the argument of the energy function), which is given by

$$U(\mathbf{w}) = \mathbf{w}^T \Psi^T \mathbf{J} \Psi \mathbf{w} + T \mathbf{w}^T \mathbf{A} \mathbf{w}, \quad (12)$$

where $\mathbf{A} = \text{diag}(\alpha_1, \dots, \alpha_{N^2})$.

Then, the *a priori* distribution of \mathbf{w} is given by

$$p(\mathbf{w}|\mathbf{A}) \propto \exp\left(-\frac{1}{T} \mathbf{w}^T \Psi^T \mathbf{J} \Psi \mathbf{w} - \mathbf{w}^T \mathbf{A} \mathbf{w}\right). \quad (13)$$

Obviously, when $T \rightarrow \infty$ (high temperature and no correlation), (13) degrades to standard Bayesian compressed sensing.

IV. COMPRESSED SENSING BASED RECONSTRUCTION

In this section, we discuss how to reconstruct the geographical-spectral image from random reports via Bayesian compressed sensing. We first introduce the mechanism of random sampling. Then, we derive equations solving Bayesian compressed sensing. Due to the complexity of the equations, we proposed a post processing procedure to incorporate the spatial correlations.

A. Random Sampling

We assume that M secondary users with random locations report their observations about primary users' activity intensity. We ignore the procedure of transmission of reports, as well as quantization errors. Then, the M -dimensional observation vector at the processing center is given by

$$\mathbf{y} = \tilde{\Psi} \mathbf{w} + \mathbf{n}, \quad (14)$$

where the $M \times N$ matrix $\tilde{\Psi}$ is obtained from the corresponding rows of Ψ and \mathbf{n} is white Gaussian noise with zero mean and variance σ_n^2 .

B. Bayesian Compressed Sensing

1) Marginal Likelihood: We follow a derivation similar to that in [15] to obtain the algorithm of Bayesian compressed sensing for image reconstruction. Essentially, the procedure of reconstruction is to learn the hyperparameters $\{\alpha_i\}_{i=1,\dots,N^2}$ from the observations at the processing center. Following the

same argument as in [15], the hyperparameters are obtained by maximizing the marginal likelihood, which is given by

$$p(\mathbf{y}|\mathbf{A}) = \int_{\mathbb{R}^{N^2}} p(\mathbf{y}|\mathbf{w}) p(\mathbf{w}|\mathbf{A}) d\mathbf{w}, \quad (15)$$

where $p(\mathbf{w}|\mathbf{A})$ is given by (13) and

$$p(\mathbf{y}|\mathbf{w}) = \frac{1}{(\sqrt{2\pi}\sigma_n^2)^{N^2}} \exp\left(-\frac{\|\mathbf{y} - \tilde{\Psi} \mathbf{w}\|^2}{\sigma_n^2}\right). \quad (16)$$

It is easy to verify that (15) is equal to (the derivation is omitted due to limited space)

$$p(\mathbf{y}|\mathbf{A}) = (2\pi)^{-N^2/2} |\mathbf{C}|^{-1/2} \exp\left(-\frac{1}{2} \mathbf{y}^T \mathbf{C}^{-1} \mathbf{y}\right), \quad (17)$$

where

$$\mathbf{C} = \sigma_n^2 \mathbf{I} + \tilde{\Psi} \mathbf{B}^{-1} \tilde{\Psi}^T \mathbf{y}, \quad (18)$$

and

$$\mathbf{B} = \frac{1}{T} \tilde{\Psi}^T \mathbf{J} \tilde{\Psi} + \mathbf{A}. \quad (19)$$

2) Learning Hyperparameters: Adopting the same argument as in [15], we learn the hyperparameters $\{\alpha_n\}_{n=1,\dots,N^2}$ by maximizing $p(\mathbf{y}|\mathbf{A})$ in (17). We can take derivative on the right hand side of (17) and letting the derivative to be zero, thus obtaining the following necessary condition for the hyperparameters maximizing the marginal likelihood:

$$(\mathbf{B}^{-1})_{ii} - \mu_i^2 - \Sigma_{ii} = 0, \quad (20)$$

where

$$\Sigma = \left(\frac{1}{\sigma_n^2} \tilde{\Psi}^T \tilde{\Psi} + \mathbf{B}\right)^{-1}, \quad (21)$$

and

$$\mu = \frac{1}{\sigma_n^2} \Sigma \tilde{\Psi}^T \mathbf{y}. \quad (22)$$

The detailed derivation is omitted due to limited space. Note that, similarly to [15], (20) can also be obtained from Expectation Maximization (EM). The derivation is omitted due to limited space.

Unfortunately, we are still unable to find an efficient algorithm to solve equation (20), where the main difficulty is the inversion of matrix \mathbf{B} . In traditional Bayesian compressed sensing, \mathbf{B} is diagonal, thus facilitating the computation. However, we have not found a good approach to tackle the inversion of \mathbf{B} .

3) Recovering Image: Once we obtain $\{\alpha_i\}_{i=1,\dots,N^2}$, we can find the maximum likelihood estimation of \mathbf{w} . It has been shown in [15] that \mathbf{w} is Gaussian distributed with variance matrix Σ and μ . Therefore, the maximum likelihood estimation of \mathbf{w} is given by

$$\mathbf{w}^* = \mu. \quad (23)$$

Then, the image estimation is given by

$$\hat{\mathbf{x}} = \Psi \mu. \quad (24)$$

4) *Post Processing*: Although it is difficult to incorporate the energy function for modeling spatial correlations into Bayesian compressed sensing simultaneously, we can carry out Bayesian compressed sensing with infinite temperature and then incorporate the spatial correlation in a post processing stage.

Denote by $\hat{\mathbf{x}}$ the reconstructed image using standard Bayesian compressed sensing. Then, we carry out the post processing by the following optimization:

$$\min_{\mathbf{x}} \sum_{i \sim j} (x_i - x_j)^2 + \omega \sum_i (x_i - \hat{x}_i)^2, \quad (25)$$

where ω is a weighting factor to balance the spatial correlation and the belief on the results obtained from Bayesian compressed sensing. It is easy to verify that the solution to (25) is given by the following equations:

$$(N_i + \omega) x_i - \sum_{j \sim i} x_j = \omega \hat{x}_i, \quad i = 1, \dots, N^2, \quad (26)$$

where N_i is the number of neighbors of point i . Then, the optimal solution is output as the reconstructed image.

V. NUMERICAL RESULTS

In this section, we first explain the approach of generating geographical-spectral pattern from pathloss and shadow fading models. Then, we show examples of reconstruction with respect to different sampling rates, as well as the average relative error of reconstructions.

A. Generation of Geographical-Spectral Images

In numerical simulations, we generate geographical-spectral images using Procedure 1. We assume a $10\text{km} \times 10\text{km}$ area and drop P primary users randomly within this area. For each location, we use the sum of average interference power from primary users (only path loss and shadow fading are considered since the effect of fast fading can be smoothed out) to represent the intensity of interruptions by assuming all primary users are active. The whole area is divided into a 10×10 grid and the pixel at each grid is obtained by averaging the interference power within this grid, thus forming a 10×10 image.

B. Linear Transformation

We use two-dimensional discrete cosine transform (DCT) for the linear transform i.e.

$$\begin{aligned} \mathbf{W}_{k_1, k_2} &= \sum_{n_1=0}^{N-1} \sum_{n_2=0}^{N-1} \mathbf{X}_{n_1, n_2} \cos \left[\frac{\pi}{N_1} \left(n_1 + \frac{\pi}{2} \right) k_1 \right] \\ &\times \cos \left[\frac{\pi}{N_2} \left(n_2 + \frac{\pi}{2} \right) k_2 \right]. \end{aligned} \quad (27)$$

Procedure 1 Procedure of Generating Geographical-Spectral Images

```

1: for i=1:number of images do
2:   Randomly distribute  $M$  primary users in a square area.
3:   for every location do
4:     for every primary user do
5:       Compute path loss using  $L = 28.6 + 35 \log_{10} d(\text{dB})$ , where  $d$  is distance measured by meters.
6:       Generate random shadow fading gain using lognormal distribution with variance 8.9dB.
7:       Compute receiver power from the primary user (we assume that the transmit power of each primary user is 200mW).
8:       Accumulate the total receiver power.
9:   end for
10:  Record the total received power at the location.
11: end for
12:  Generate the current image.
13:  Divide the image into grids and average over each grid.
14: end for
15: Output all images.

```

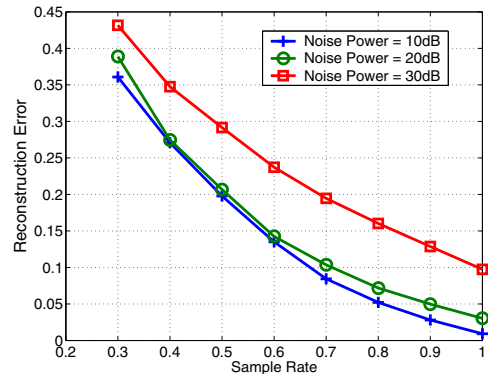


Fig. 2: Relative error of reconstruction with respect to different noise powers.

C. Impact of Noise Power

In this subsection, we assume that $P = 10$, i.e. there are 10 primary users randomly distributed within the area. The image is reconstructed using Bayesian compressed sensing with $T = \infty$. Fig. 2 shows the relative error of reconstruction with respect to different noise powers, which is defined as

$$e = \frac{\|\hat{\mathbf{x}} - \mathbf{x}\|}{\|\mathbf{x}\|}, \quad (28)$$

where $\hat{\mathbf{x}}$ is the reconstructed image in vector form. We observe that, when the noise power ranges from 10dB to 20dB, the reconstruction precision changes only marginally. However, when the noise power is large (30dB), the reconstruction precision is significantly impaired even when observations from all locations are collected.

D. Impact of the Number of Primary Users

Fig. 3 shows the relative error of reconstruction with respect to different numbers of primary users dropped within the area (the noise power is fixed at 10dB). We observe that the reconstruction precision is decreased as more primary users emerge while the degradation is marginal.

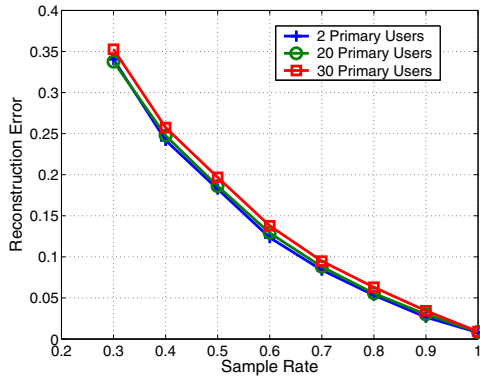


Fig. 3: Relative error of reconstruction with respect to different numbers of primary users.

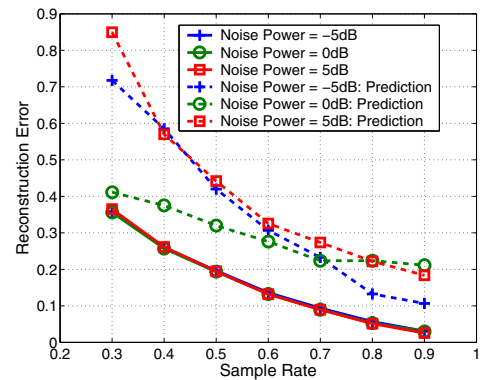


Fig. 4: Performance of prediction with noise power ranging from -5dB to 5dB.

E. Unmeasured Locations

Since the main purpose of recovering the geographical-spectral pattern is to predict the activity of primary users at locations without reports, we test the reconstruction error at unmeasured locations and the performance is shown in Fig. 4 (noise power ranging from -5dB to 5dB). We observe that the reconstruction errors at the unmeasured locations are significantly higher than the reconstruction error averaged over the whole area. However, when the noise power is small, we can still achieve reasonable prediction precision at these locations.

F. Impact of Post Processing

Fig. 5 shows the performance of geographical-spectral image reconstruction with post processing ($\omega = 10$). We observe that, for $\omega = 10$, the post processing improves the performance when the reconstruction error is large.

VI. CONCLUSIONS

We have proposed the concept of geographical-spectral pattern of interruptions from primary users and discussed its applications in the upper layer issues like routing and congestion control in cognitive radio networks. For single-channel case, the pattern can be considered as an image while it can be modeled as hyperspectral images for multi-channel

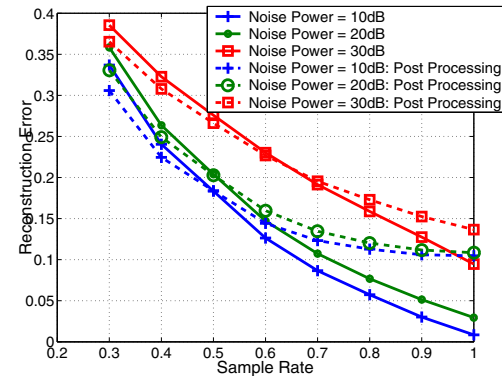


Fig. 5: Performance of post processing with $\omega = 10$.

case. We have proposed to recover the image (pattern) from reports of secondary users, like reconstructing an image from random samples. To capture the smoothness of the image, we have used Gibbs random fields to model the correlations between neighboring locations via a proper energy function. Hyperparameters are incorporated into the energy function to facilitate Bayesian compressed sensing. To alleviate the difficulty of Bayesian compressed sensing with correlation modeling, we have proposed a post processing mechanism to incorporate the information about spatial correlation. We have used numerical simulations to demonstrate the performance of the proposed schemes.

REFERENCES

- [1] S. Biswas and R. Morris, "ExOR: Opportunistic multi-hop routing for wireless networks," in *Proc. of ACM SIGCOMM*, 2005.
- [2] E. J. Candès, J. Romberg and T. Tao, "Robust uncertainty principles: Exact signal reconstruction from highly incomplete frequency information," *IEEE Trans. Inform. Theory*, Vol. 52, no.2, pp. 489- 509, Feb. 2006.
- [3] K. R. Chowdhury, M. D. Felice and I. F. Akyildiz, "TP-CRAHN: A transport protocol for cognitive radio ad hoc networks," in *Proc. of IEEE Conference on Computer Communications (INFOCOM)*, 2009.
- [4] D. L. Donoho, "Compressed sensing," *IEEE Trans. Inform. Theory*, Vol. 52, no.4, pp. 1289-1306, April 2006.
- [5] H. Grahn and P. Geladi, *Techniques and Applications of Hyperspectral Image Analysis*, Wiley, 2007.
- [6] J. M. Hammersley and P. Clifford, "Markov field on finite graphs and lattices," unpublished.
- [7] R. A. Horn and C. R. Johnson, *Topics in Matrix Analysis*, Cambridge University Press, Cambridge, UK, 1991.
- [8] S. Ji, Y. Xue and L. Carin, "Bayesian compressive sensing," *IEEE Trans. on Signal Processing*, vol. 56, no.6, pp.2346-2356, June 2008.
- [9] H. Kushwaha, Y. Xing, R. Chandramouli and H. Heffes, "Reliable multimedia transmission over cognitive radio networks using Fountain codes," *Proceedings of the IEEE*, vol.96, no.1, pp.155-165, Jan. 2008.
- [10] D. Landgrebe, "Hyperspectral image data analysis as a high dimensional signal processing problem," *IEEE Signal Processing Magazine*, vol.19, pp.17-28, 2002.
- [11] S. Z. Li, *Markov Random Field Modeling in Image Analysis*, Springer, 2009.
- [12] J. Mitola, "Cognitive radio for flexible mobile multimedia communications," in *Proc. IEEE Int. Workshop Mobile Multimedia Communications*, pp. 3-10, 1999.
- [13] M. Pan, R. Huang and Y. Fang, "Cost design for opportunistic multi-hop routing in cognitive radio networks," in *Proc. of IEEE Milcom*, 2008.
- [14] H. Rue and L. Held, *Gaussian Markov Random Fields: Theory and Applications*, Chapman & Hall/CRC, 2005.
- [15] M. E. Tipping, "Sparse Bayesian learning and the relevance vector machine," *Journal of Machine Learning Research*, vol.1, pp.211-244, 2001.